www.nature.com/eye

CLINICAL STUDY

Agreement between image grading of conventional (45°) and ultra wide-angle (200°) digital images in the macula in the Reykjavik eye study

A Csutak[1,2], I Lengyel[3], F Jonasson[4,5], I Leung[1], A Geirsdottir[4], W Xing[1] and T Peto[1]

[1]Moorfields Eye Hospital, London, England

[2]University of Debrecen Medical and Health Science Centre, Debrecen, Hungary

[3]UCL Institute of Ophthalmology, London, England

[4]Landspitali University Hospital, Reykjavik, Iceland

[5]Faculty of Medicine University of Iceland, Reykjavik, Iceland

Correspondence: T Peto, Head of Reading Centre, Department of Research and Development, Moorfields Eye Hospital NHS Foundation Trust, 162 City Road, London EC1V 2PD, UK
Tel: +44 207 566 2815; Fax: +44 207 608 6925.
E-mail: Tunde.Peto@moorfields.nhs.uk

Received: 31 December 2009
Accepted in revised form: 30 April 2010
Published online: 4 June 2010

Abstract

Purpose **To establish the agreement between image grading of conventional (45°) and ultra wide-angle (200°) digital images in the macula.**
Methods **In 2008, the 12-year follow-up was conducted on 573 participants of the Reykjavik Eye Study. This study included the use of the Optos P200C AF ultra wide-angle laser scanning ophthalmoscope alongside Zeiss FF 450 conventional digital fundus camera on 121 eyes with or without age-related macular degeneration using the International Classification System. Of these eyes, detailed grading was carried out on five cases each with hard drusen, geographic atrophy and chorioretinal neovascularisation, and six cases of soft drusen. Exact agreement and κ-statistics were calculated.**
Results **Comparison of the conventional and ultra wide-angle images in the macula showed an overall 96.43% agreement ($\kappa = 0.93$) with no disagreement at end-stage disease; although in one eye chorioretinal neovascularisation was graded as drusenoid pigment epithelial detachment. Of patients with drusen only, the exact agreement was 96.1%. The detailed grading showed no clinically significant disagreement between the conventional 45° and 200° images.**
Conclusions **On the basis of our results, there is a good agreement between grading conventional and ultra wide-angle images in the macula.**
Eye (2010) **24,** 1568–1575; doi:10.1038/eye.2010.85; published online 4 June 2010

Keywords: age-related macular degeneration; image grading; geographic atrophy; choroidal neovascularisation; drusen; imaging

Introduction

Fundus imaging is frequently used to document and monitor retinal lesions. Both film and digital images are widely used and the two show good agreement.[1–4] The 30–60° photographic field has become the standard for most studies. The magnification provided by these images is usually adequate to determine most lesions including age-related maculopathy and macular degeneration (ARM and AMD, respectively).[5] AMD is a major cause of visual loss in the elderly[6] that involves the retinal pigment epithelium (RPE), Bruch's membrane, choroidal vasculature and photoreceptors. Although ARM and AMD has been described for over 100 years, details of internationally accepted grading systems are relatively new and not necessarily universally used.[7] However, determining the aetiology of ARM is important for the identification of risk factors.[8] Validation and calibration of grading systems is difficult because clinicians, epidemiologist, and pathologist use different definitions and even different names for ARM and AMD.[7]

ARM and AMD, similar to several other retinal disorders, show distinct topographical patterns of pathology. Although diagnosis relies on changes in the macula, there are many age-related changes in the periphery that may influence the development of macular lesions or the macular pathology itself may trigger peripheral changes[9] that could influence treatment strategies. Therefore, monitoring changes in the periphery may become an indispensible tool to fully understand ARM and AMD disease aetiology. To obtain wide-field images, standard protocols such as the seven

field images were generated in the past. This allowed the visualisation of approximately 75° fields. Recently, the P200C AF scanning laser ophthalmoscope (OPTOS PLC) was introduced that allows the rapid (0.25 s), wide-angle (up to 200°) imaging of the retina in a single image. This image can be obtained with or without mydriasis.

The main purpose of this article was to determine the feasibility to use ultra wide-angle (200°) digital imaging to record phenotypic variation of AMD in the macula of eyes from the 12-year follow-up of Reykjavik Eye Study.

Materials and methods

The Reykjavik Eye Study includes a random sample from the Reykjavik population census 50 years and older in 1996, in which 1045 persons participated, all having an eye examination and stereo fundus photography using films.[10] In 2008, the 12-year follow-up was conducted in which 573 persons participated, that is, 73% of the survivors. Participants were photographed using the P200C AF, an ultra wide-angle (200°) scanning laser ophthalmoscope that was operated by an Imaging Team provided by OPTOS and supervised by the Reading Centre of Moorfields Eye Hospital (MEHRC). The 45° fovea centred macular photographs were taken by a ZEISS FF 450 digital camera, operated by trained senior nurses of the Reykjavik Hospital Medical Retina Clinic and supervised in part by the MEHRC. Both conventional digital and ultra wide-angle images were taken through pharmacologically dilated pupils.

Tenets of the Declaration of Helsinki were followed. Ethical approvals were obtained from the Data Protection Authority and the National Bio-Ethics Committee in Iceland. Signed informed consent was obtained from each participant. The digital images were sent to the MEHRC with a unique ID number displayed on all photographs. These ID numbers were used to identify patients and grading records in the Reykjavik Eye Study.

For our current protocol, 121 eyes were selected from the 12-year follow-up, and care was taken to cover the whole spectrum of ARM and AMD. Images were graded in random order without access to clinical information. Both conventional and ultra wide-angle images were graded using the Optos V2 vantage DX review software that allows the automatic fitting of a standard grid after manually defining the centres of the fovea and the optic disc. This definition of grading grid ensured that the very same macular areas were graded in both image modalities (see examples of corresponding images in Figure 1). Standard circles were used to measure the drusen and lesions sizes. Only abnormalities related to ARM and AMD were graded. Both conventional and ultra wide-angle images were phenotyped by the same person using the categories of the International Classification (IC):[7] hard and soft drusen, geographic atrophy (GA), and chorioretinal neovascularisations (CNV) were identified. Intra-observer agreement was calculated once the images were regarded after a minimum of 14 days interval.

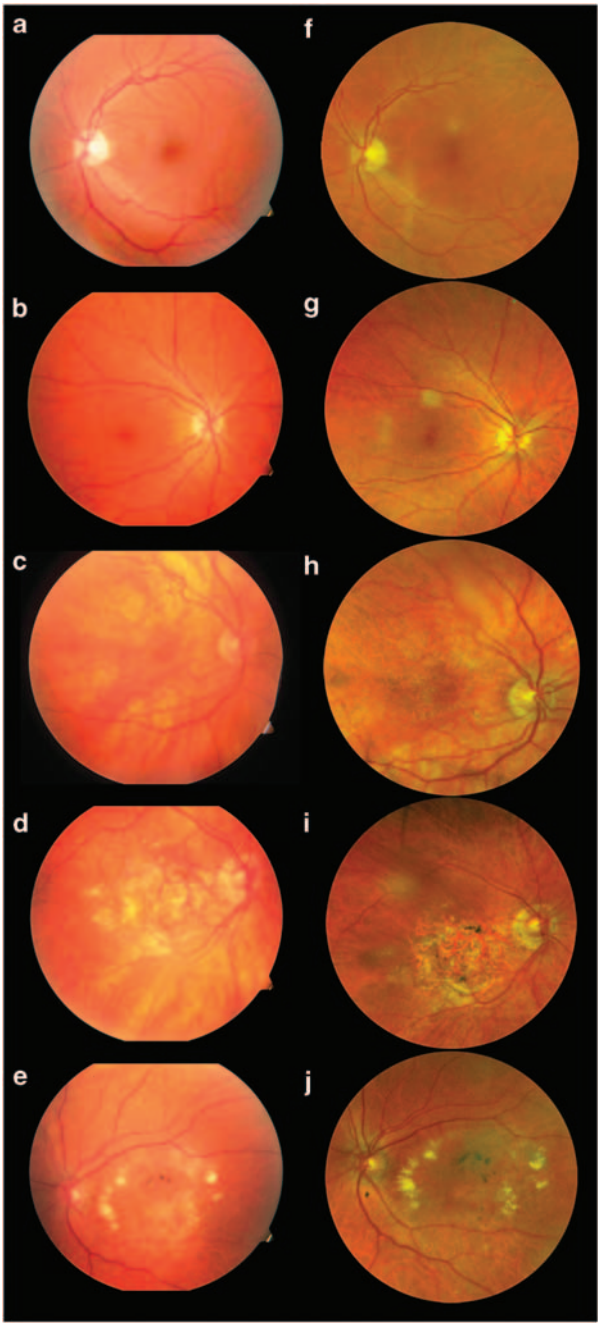

Figure 1 Corresponding images of the macula of the same eye taken by the Zeiss FF 450 conventional 45° digital fundus camera (a–e) and, after fitting landmarks on the images and cropping, Optos P200C AF ultra wide-angle laser scanning ophthalmoscope (f–j): (a–f) no pathology; (b–g) early ARM; (c–h) early AMD; (d–i) choroidal neovascularisation; (e–j) geographic atrophy.

Of the phenotyped images, detailed grading was conducted on five cases each with hard drusen, GA and CNV, and six cases of soft drusen (21 eyes in total), on both imaging modalities using the Optos V2 vantage DX review software by individually recording all drusen types and sizes for all three zones of the IC grading, together with recording RPE changes, characteristics, and size of CNV and GA. This represented the same grading protocol that was used as for the baseline and the 5-year follow-up of the Reykjavik Eye Studies to allow incidence estimates at the later date.[10,11] Incidental finding were commented on the grading form. Intra- and inter-observer agreement was calculated once the images were regarded after 14 days by the same or by another certified grader.

Exact agreement and κ-statistics were calculated between intra- and inter-graders.[12] The κ-statistic was interpreted as follows: $\kappa<0$, poor agreement; κ-values 0–0.2, 'slight'; 0.21–0.40, 'fair'; 0.41–0.60, 'moderate'; 0.61–0.8, 'substantial'; and $\kappa>0.81$, 'almost perfect agreement'.[12] Statistical analysis was performed using Stata 9.0 (StataCorp LP, College Station, TX, USA).

Results

To assess the feasibility to use the P200C AF images for grading for ARM and AMD in the macula we used a two-step analysis. First, macular pathologies were graded both on ultra wide-angle and conventional digital images from 121 (10.56% of total) eyes by one grader. Of these, nine conventional digital images were not gradable. All ultra wide-angle images were sufficiently good quality for grading. After comparison of the 112 remaining eyes, there was a 96.43% agreement ($\kappa=0.93$) in the overall diagnosis of end-stage diseases (19 eyes). The only disagreement came from one eye that was graded as CNV on the ultra wide-angle image and drusenoid pigment epithelial detachment (PED) on the conventional digital image. Seventy-seven eyes were graded as drusen only on conventional digital images and 74 on the P200C AF images. Disagreement came from three eyes that were graded as normal on the P200C AF images (exact agreement 96.1%, $\kappa=0.00$). There were no disagreements in grading normal fundus images (16 eyes).

In the second step detailed grading was carried out by two independent graders on five cases each with hard drusen, GA and CNV, and six cases of soft drusen using the International Classification used for both the baseline and the 5-year follow-up of the Reykjavik Eye Study. Grading categories, exact agreement and κ-statistics are listed in Tables 1-3. As there was no clinically relevant difference between the two graders, their detailed grading was collapsed and the grading of the two imaging modalities were compared. The agreement between the two imaging modalities was overall high in all categories, except grading hard ($<63\,\mu$m), intermediate soft (63–125 μm) drusen, and the area covered by drusen. In these categories the agreement ranged between moderate to low (Table 1). Inter-grader reliability for both image modalities was generally high, except for small hard drusen ($<63\,\mu$m) and for intermediate to soft drusen (63–125 μm) (Table 2). The intra-grader reliability was calculated by re-grading the images at least 14 days after the first grading. Intra-grader reliability was high in all categories (Table 3), except for some categories of drusen (Table 3). This disagreement was consistently driven by only one case, which on first grading was deemed not gradable due to image quality, but graded as normal at re-grading.

Discussion

Digital fundus photography has become a sensitive and reliable tool in grading abnormalities in ARM and AMD.[4] Nowadays clinicians are aided by and document their diagnoses using this 'gold standard'. Therefore, it is imperative that new digital imaging systems are compared with the well accepted and characterised conventional digital fundus images. In this study, we compared the grading of macular pathologies in ultra wide-angle (200°) scanning laser ophthalmoscope-generated digital images with non-stereoscopic conventional digital fundus images (45°) of eyes of the 12-year follow-up of the Reykjavik Eye Study. The comparison showed good agreement for ARM and AMD characteristics between the two imaging modalities.

The P200C AF imaging system (Optos, Dunfermline, UK) is a scanning laser ophthalmoscope that captures a wide-field retinal image up to 200°. Images can be captured in 250 ms allowing the rapid imaging of even the vulnerable patients often even without mydriasis. The P200C AF uses red (633 nm) and green (532 nm) lasers, which are reflected off a large concave elliptical mirror. The resulting images are displayed as red only, green only, and a combined red–green 'false colour' images. Each image has a resolution of 3000 by 3000 pixels. The P200C AF is the latest in a series of devices that use a common imaging platform to document a wide range of abnormalities in the retina. Although this is the first study with the P200C AF device, an earlier device in this series, the P200 has been used in previous studies.[13–16]

Ultra wide-angle images had not previously been used to grade changes associated with ARM or AMD, although the presence of pathological abnormalities in the macula had been described.[17] In this study, we

Table 1 Agreement between grading conventional (45) and ultra wide-angle (200) digital images

	Zone 1	*Zone 2*	*Zone 3*
Drusen <63 μm (hard drusen)	62%, $\kappa = 0.26$, $P = 0.0027$	60%, $\kappa = 0.37$, $P = 0.0003$	38%, $\kappa = 0.15$, $P = 0.035$
Drusen 63–125 μm (intermediate soft drusen)	79%, $\kappa = 0.54$, $P < 0.0001$	83%, $\kappa = 0.75$, $P < 0.0001$	74%, $\kappa = 0.62$, $P < 0.0001$
Drusen 125–250 μm (large semisolid drusen distinct, subconfluent, confluent)	95, 95, 95%, $\kappa = 0.0$, $\kappa = 0.0$, $\kappa = 0.0$, NP, NP, NP	83, 93, 98%, $\kappa = 0.29$, $\kappa = 0.36$, $\kappa = 0.84$, $P = 0.015$, $P = 0.0079$, $P < 0.0001$	91, 95, 100%, $\kappa = 0.69$, $\kappa = 0.81$, $\kappa = 1.0$, $P < 0.0001$, $P < 0.0001$, $P < 0.0001$
Drusen 250–500 μm (large semisolid drusen distinct, subconfluent, confluent)	95, 95, 95%, $\kappa = 0.0$, $\kappa = 0.0$, $\kappa = 0.0$, NP, NP, NP	100, 100, 95%, NP, NP, $\kappa = 0.00$, NP, NP, $P < 0.0001$	100, 98, 98%, $\kappa = 1.0$, $\kappa = 0.00$, $\kappa = 0.00$, $P < 0.0001$, $P = 0.5$, $P = 0.5$
Drusen >500 μm (large semisolid drusen distinct, subconfluent, confluent)	95, 95, 93%, $\kappa = 0.0$, $\kappa = 0.0$, $\kappa = -0.02$, NP, NP, $P = 0.59$	100, 95, 95%, NP, $\kappa = -0.02$, $\kappa = 0.48$ NP, $P = 0.56$, $P < 0.0001$	100, 98, 98%, NP, $\kappa < 0.01$, $\kappa = 0.66$ NP, $P = 0.5$, $P < 0.0001$
Crystalline drusen	95%, $\kappa = 0.65$, $P < 0.0001$	90%, $\kappa = -0.04$, $P = 0.61$	98%, $\kappa = 0.88$, $P < 0.0001$
Serogranular drusen	95%, $\kappa = 0.49$, $P < 0.0001$		
Hyperpigmentation (presence)	95% $\kappa = 0.84$ $P < 0.0001$	88% $\kappa = 0.61$ $P < 0.0001$	91%, $\kappa = 0.47$, $P < 0.0001$
Hyperpigmentation (type)	95% $\kappa = 0.83$ $P < 0.0001$	100% NP NP	91%, $\kappa = 0.46$, $P < 0.0001$
Hypopigmentation (presence)	100% $\kappa = 1.0$ $P < 0.0001$	100% NP NP	100%, NP, NP
Geographic atrophy (presence)	100% $\kappa = 1.0$, $P < 0.0001$	98%, $\kappa = 0.93$, $P < 0.0001$	95%, $\kappa = 0.88$, $P < 0.0001$
Neovascular AMD (presence)	95%, $\kappa = 1.0$, $P < 0.0001$	86%, $\kappa = 0.52$, $P < 0.0001$	95%, $\kappa = 0.65$, $P < 0.0001$
Neovascular AMD (features)	98%, $\kappa = 0.79$, $P < 0.0001$	98%, $\kappa = 0.79$, $P < 0.0001$	100%, $\kappa = 1.0$, $P < 0.0001$
Neovascular AMD (scar/fibrous)	100%, $\kappa = 1.0$, $P < 0.0001$	91% $\kappa = 0.56$ $P < 0.0001$	95% $\kappa = 0.00$ NP
Neovascular AMD (retinal haemorhage)	98%, $\kappa = 0.00$, $P = 0.5000$	98%, $\kappa = 0.79$, $P < 0.0001$	100%, $\kappa = 1.0$, $P < 0.0001$
Area covered by neovascular AMD		86%, $\kappa = 0.62$, $P < 0.0001$	
Area covered by geographic atrophy		88% $\kappa = 0.74$, $P < 0.0001$	
Area covered by drusen		67%, $\kappa = 0.43$, $P < 0.0001$	
Predominant phenotype		95%, $\kappa = 0.94$, $P < 0.0001$	
Image quality		59%, $\kappa = 0.30$, $P = 0.0018$	

Abbreviation: NP, not possible to compute.

Table 2 Inter-observer variability

	Zone 1	*Zone 2*	*Zone 3*
Drusen <63 μm (hard drusen)	67%, $\kappa=0.36$, $P<0.0001$	64%, $\kappa=0.45$, $P<0.0001$	62%, $\kappa=0.46$, $P<0.0001$
Drusen 63–125 μm (intermediate soft drusen)	83%, $\kappa=0.64$, $P<0.0001$	74%, $\kappa=0.60$, $P<0.0001$	74%, $\kappa=0.62$, $P<0.0001$
Drusen 125–250 μm (large semisolid drusen distinct, subconfluent, confluent)	100, 100, 100%, $\kappa=1.0$, $\kappa=1.0$, $\kappa=1.0$, $P<0.0001$, $P<0.0001$, $P<0.0001$	79, 93, 98%, $\kappa=0.08$, $\kappa=0.36$, $\kappa=0.84$, $P=0.257$, $P=0.0079$, $P<0.0001$	71, 91, 95%, $\kappa=0.18$, $\kappa=0.61$, $\kappa=0.00$, $P=0.02$, $P<0.0001$, NP
Drusen 250–500 μm (large semisolid drusen distinct, subconfluent, confluent)	100, 100, 100%, $\kappa=1.0$, $\kappa=1.0$, $\kappa=1.0$, $P<0.0001$, $P<0.0001$, $P<0.0001$	100, 100, 95%, NP, NP, $\kappa=0.00$, NP, NP, NP	95, 98, 98%, $\kappa=0.0$, $\kappa=0.00$, $\kappa=0.00$, NP, $P=0.5$, $P=0.5$
Drusen >500 μm (large semisolid drusen distinct, subconfluent, confluent)	100, 100, 97%, $\kappa=1$, $\kappa=1$, $\kappa=0.66$, $P<0.0001$, $P<0.0001$, $P<0.0001$	100, 95, 91%, NP, $\kappa=-0.024$, $\kappa=-0.018$, NP, $P=0.56$, $P=0.61$	100, 98, 93%, NP, $\kappa=0.000$, $\kappa=0.00$ NP, $P=0.5$, NP
Crystalline drusen	100%, $\kappa=1.0$ $P<0.0001$	95%, $\kappa=0.48$, $P<0.0001$	98%, $\kappa=0.87$, $P<0.0001$
Serogranular drusen	95%, $\kappa=0.49$, $P<0.0001$		
Hyperpigmentation (presence)	91%, $\kappa=0.67$, $P<0.0001$	93%, $\kappa=0.77$, $P<0.0001$	95%, $\kappa=0.73$, $P<0.0001$
Hyperpigmentation (type)	91%, $\kappa=0.67$, $P<0.0001$	93%, $\kappa=0.77$, $P<0.0001$	95%, $\kappa=0.73$, $P<0.0001$
Hypopigmentation (presence)	95%, NP, NP	100%, NP, NP	100%, NP, NP
Geographic atrophy (presence)	100%, $\kappa=1.0$, $P<0.0001$	98%, $\kappa=0.93$, $P<0.0001$	91%, $\kappa=0.77$, $P<0.0001$
Neovascular AMD (presence)	95%, $\kappa=0.87$, $P<0.0001$	93%, $\kappa=0.75$, $P<0.0001$	95%, $\kappa=0.65$, $P<0.0001$
Neovascular AMD (features)	98%, $\kappa=0.79$, $P<0.0001$	98%, $\kappa=0.79$, $P<0.0001$	100%, $\kappa=1.0$, $P<0.0001$
Neovascular AMD (scar/fibrous)	95%, $\kappa=0.84$, $P<0.0001$	95%, $\kappa=0.78$, $P<0.0001$	95%, $\kappa=0.00$, NP
Neovascular AMD (retinal haemorhage)	98%, $\kappa=0.000$, $P=0.5$	98%, $\kappa=0.79$, $P<0.0001$	100%, $\kappa=1.0$, $P<0.0001$
Area covered by neovascular AMD		93%, $\kappa=0.81$, $P<0.0001$	
Area covered by geographic atrophy		95%, $\kappa=0.89$, $P<0.0001$	
Area covered by drusen		79%, $\kappa=0.63$ $P<0.0001$	
Predominant phenotype		95% $\kappa=0.94$, $P<0.0001$	
Image quality		55%, $\kappa=0.23$, $P=0.0103$	

Abbreviation: NP, not possible to compute.

Table 3 Inra-observer variability

	Zone 1	*Zone 2*	*Zone 3*
Drusen <63 μm (hard drusen)	76%, $\kappa=0.59$, $P<0.0001$	81%, $\kappa=0.71$, $P=0.0001$	76%, $\kappa=0.67$, $P<0.0001$
Drusen 63–125 μm (intermediate soft drusen)	95%, $\kappa=0.90$, $P<0.0001$	81%, $\kappa=0.73$, $P<0.0001$	86%, $\kappa=0.79$, $P<0.0001$
Drusen 125–250 μm (large semisolid drusen distinct, subconfluent, confluent)	100; 100; 100%, $\kappa=1.00$; $\kappa=1.00$; $\kappa=1.00$, $P<0.0001$; $P<0.0001$; $P<0.0001$	95, 90, 88%, $\kappa=-0.01$, $\kappa=-0.02$, $\kappa=-0.02$, $P=0.5628$, $P=0.6105$, $P=0.6287$	93, 79, 83%, $\kappa=-0.02$, $\kappa=-0.02$, $\kappa=-0.02$, $P=0.5895$, $P=0.6883$, $P=0.6603$
Drusen 250–500 μm (large semisolid drusen distinct, subconfluent, confluent)	100, 98, 100% $\kappa=1.00$, $\kappa=0.66$, $\kappa=1.00$ $P<0.0001$, $P<0.0001$, $P<0.0001$	95, 95, 98%, $\kappa=-0.01$, $\kappa=0.00$, $\kappa=0.00$, $P=0.5628$, $P=$NP, $P=0.50$	95, 95, 98%, $\kappa=-0.0120$, $\kappa=0.00$, $\kappa=0.00$, $P=0.5628$, $P=$NP, $P=0.5$
Drusen >500 μm (large semisolid drusen distinct, subconfluent, confluent)	100, 100, 98%, $\kappa=1.00$, $\kappa=1.00$, $\kappa=0.66$, $P<0.0001$, $P<0.0001$, $P<0.0001$	TFC, 98, 98%, NP, $\kappa=0.00$, $\kappa=0.49$, NP, $P=0.5$, $P<0.0001$	TFC, TFC, TFC, $\kappa=$NP, $\kappa=$NP $\kappa=$NP, $P=$NP, $P=$NP, $P=$NP
Hyperpigmentation (presence)	100%, $\kappa=1.00$, $P<0.0001$	98%, $\kappa=0.91$, $P<0.0001$	100%, $\kappa=1.00$, $P<0.0001$
Hyperpigmentation (type)	100%, $\kappa=1.00$, $P<0.0001$	98%, $\kappa=0.91$, $P<0.0001$	98%, $\kappa=0.86$, $P<0.0001$
Hypopigmentation (presence)	TFC, NP, NP	TFC, NP, NP	98%, $\kappa=0.00$, $P=0.5$
Geographic atrophy (presence)	100%, $\kappa=1.00$, $P<0.0001$	100%, $\kappa=1.00$, $P<0.0001$	98%, $\kappa=0.93$, $P<0.0001$
Neovascular AMD (presence)	100%, $\kappa=1.00$, $P<0.0001$	98%, $\kappa=0.93$, $P<0.0001$	100.00%, $\kappa=1.00$, $P<0.0001$
Neovascular AMD (features)	100%, $\kappa=1.00$, $P<0.0001$	100%, $\kappa=1.00$, $P<0.0001$	98%, $\kappa=0.74$, $P<0.0001$
Neovascular AMD (scar/fibrous)	98%, $\kappa=0.93$, $P<0.0001$	98%, $\kappa=0.91$, $P<0.0001$	100%, $\kappa=1.00$, $P<0.0001$
Neovascular AMD (retinal haemorhage)	100%, $\kappa=1.00$, $P<0.0001$	98%, $\kappa=0.79$, $P<0.0001$	98%, $\kappa=0.79$, $P<0.0001$
Area covered by neovascular AMD		100%, $\kappa=1.0$, $P<0.0001$	
Area covered by geographic atrophy		98%, $\kappa=0.94$, $P<0.0001$	
Area covered by drusen		95%, $\kappa=0.92$, $P<0.0001$	
Predominant phenotype		100%, $\kappa=1.00$, $P<0.0001$	
Image quality		52%, $\kappa=0.30$, $P=0.0005$	

Abbreviations: NP, not possible to compute; TFC, too few rating categories.

compared grading of ultra wide-angle images and conventional digital images using the IC system developed earlier.[7] Our first observation was that although all ultra wide-angle images were gradable, there were nine conventional images that fell short of grading standards, predominantly due to media opacities and technical difficulties with positioning the patient for long enough to take gradable images. As lasers are much less susceptible to any media opacities[18,19] and they outperform even very high resolution digital images in terms of sharpness and contrast,[20] the better image quality is perhaps not surprising. However, it must be acknowledged that new graders must learn to appreciate artifacts related to the broad depth of focus of this device, such as the presence of eyelids, eyelashes, floaters (eg, see Supplementary Figure 1), the optics and the haptics of the intraocular lens or lens opacities. Also the image, as it is generated by green and red laser lights rather than the more widely used white light illumination, is unfamiliar to graders in the first instance. In our experience, most of these aspects can be overcome or minimised with practice and good imaging techniques. The camera can accommodate wheelchairs and there is no need to move the patient, a real advantage in imaging an elderly population similar to those in the Reykjavik Eye Study. In general, imaging did not require dilation, though when seeking to obtain the best quality of images in the most elderly and fragile dilation was necessary.

The phenotype of 112 eyes in this study showed a very high level of agreement between the image modalities, suggesting that the ultra wide-angle images of the P200C AF is a reliable way to identify fundus abnormalities. This was reinforced by the detailed grading of the select 21 eyes, which again showed good agreement between the grading of the two image modalities. Intra- and inter-grader variability was low (agreement was high) in both image modalities. Only one image was interpreted differently, and graded CNV by one grader and drusenoid PED by the other. This, however, is not unacceptable as to establish the correct diagnosis for PED fluorescent angiography would have been required. Despite the fact that the graders had a short learning period to understand the P200C AF images and get enough knowledge for grading small lesions and differentiate artifacts from real abnormalities the agreement was high with high κ-values, except in those instances where there were too few categories to compare. The identification of small hard drusen gave difficulties especially at the beginning of the grading. This is reflected in the somewhat lower agreement and κ-values. This might be attributed to the similarities between drusen and pixel sizes in the ultra wide-angle images. Small hyper- and hypo-pigmentation of the RPE can be an early sign of AMD; however, grading pigment abnormalities from digital images had been shown to be difficult[4] and our study confirmed this. Neither the conventional nor the ultra wide-angle images had good enough quality or resolution to reliably grade for small pigmentary changes.

On the basis of the concordance between the conventional (45°) and ultra wide-angle (200°) digital image grading in the macula, we were satisfied that the P200C AF images document drusen, GA, and CNV similar to those of colour digital images. This builds confidence in future peripheral retinal grading of the ultra-wide field images, which might highlight important, previously unrecognised abnormalities for the fuller understanding of the development and progression of AMD pathology. How, if at all, previously reported problems with the P200[21,22] device in misdiagnosis and artefacts related to broad depth of field might affect far peripheral grading using P200C AF images remains to be evaluated.

Summary

What was known before

- Ultra wide-angle imaging is becoming more widely used and accepted in clinical settings. Yet information on its usability to detect and subsequently grade ARM and AMD pathologies has been lacking. As recent evidence points towards to the need to analyse peripheral changes in relation to ARM and AMD, it is likely that cameras capable of peripheral imaging will become part of routine clinical care.

What this study adds

- To the best of our knowledge, this study is the first to describe the agreement between conventional and ultra wide-angle digital imaging modalities in grading ARM and AMD in the macula.

Conflict of interest

The study and the fellowship of AC were part-funded by an unrestricted grant from OPTOS plc. The other authors declare no conflict of interest. The authors alone are responsible for the content and writing of this paper.

Acknowledgements

We would like to say a special thank you to the participating patients, the OPTOS clinical research team (Douglas Anderson, Anne-Marie Cairns, David Cairns, Paul Donnelly, Dana Hackman), and the medical staff at Landspitali University Hospital, Reykjavik, for their professional support. This research was supported by the Bill Brown Charitable Trust, Moorfields Eye Hospital Special Trustees, UCL Graduate School Research Projects

Fund and Mercer Fund. We also thank Professor Alan C Bird for the helpful comments. Preliminary data was presented at the ARVO 2009 meeting.

References

1 Bjornsson OM, Syrdalen P, Bird AC, Peto T, Kinge B. The prevalence of age-related maculopathy (ARM) in an urban Norwegian population: the Oslo Macular study. *Acta Ophthalmol Scand* 2006; **84**(5): 636–641.
2 van Leeuwen R, Chakravarthy U, Vingerling JR, Brussee C, Hooghart AJ, Mulder PG *et al*. Grading of age-related maculopathy for epidemiological studies: is digital imaging as good as 35-mm film? *Ophthalmology* 2003; **110**(8): 1540–1544.
3 Yannuzzi LA, Ober MD, Slakter JS, Spaide RF, Fisher YL, Flower RW *et al*. Ophthalmic fundus imaging: today and beyond. *Am J Ophthalmol* 2004; **137**(3): 511–524.
4 Scholl HP, Dandekar SS, Peto T, Bunce C, Xing W, Jenkins S *et al*. What is lost by digitizing stereoscopic fundus color slides for macular grading in age-related maculopathy and degeneration? *Ophthalmology* 2004; **111**(1): 125–132.
5 Sperduto RD, Hiller R, Podgor MJ, Palmberg P, Ferris III FL, Wentworth D. Comparability of ophthalmic diagnoses by clinical and Reading Center examiners in the Visual Acuity Impairment Survey Pilot Study. *Am J Epidemiol* 1986; **124**(6): 994–1003.
6 Leibowitz HM, Krueger DE, Maunder LR, Milton RC, Kini MM, Kahn HA *et al*. The Framingham Eye Study monograph: an ophthalmological and epidemiological study of cataract, glaucoma, diabetic retinopathy, macular degeneration, and visual acuity in a general population of 2631 adults, 1973-1975. *Surv Ophthalmol* 1980; **24**(Suppl): 335–610.
7 Bird AC, Bressler NM, Bressler SB, Chisholm IH, Coscas G, Davis MD *et al*. An international classification and grading system for age-related maculopathy and age-related macular degeneration. The International ARM Epidemiological Study Group. *Surv Ophthalmol* 1995; **39**(5): 367–374.
8 Sallo FB, Peto T, Leung I, Xing W, Bunce C, Bird AC. The International Classification system and the progression of age-related macular degeneration. *Curr Eye Res* 2009; **34**(3): 238–240.
9 Lengyel I, Tufail A, Hosaini HA, Luthert P, Bird AC, Jeffery G. Association of drusen deposition with choroidal intercapillary pillars in the aging human eye. *Invest Ophthalmol Vis Sci* 2004; **45**(9): 2886–2892.
10 Jonasson F, Arnarsson A, Sasaki H, Peto T, Sasaki K, Bird AC. The prevalence of age-related maculopathy in iceland: Reykjavik Eye Study. *Arch Ophthalmol* 2003; **121**(3): 379–385.
11 Jonasson F, Arnarsson A, Peto T, Sasaki H, Sasaki K, Bird AC. 5-year incidence of age-related maculopathy in the Reykjavik Eye Study. *Ophthalmology* 2005; **112**(1): 132–138.
12 Landis JR, Koch GG. The measurement of observer agreement for categorical data. *Biometrics* 1977; **33**(1): 159–174.
13 Kaines A, Tsui I, Sarraf D, Schwartz S. The use of ultra wide field fluorescein angiography in evaluation and management of uveitis. *Semin Ophthalmol* 2009; **24**(1): 19–24.
14 Kaines A, Oliver S, Reddy S, Schwartz SD. Ultrawide angle angiography for the detection and management of diabetic retinopathy. *Int Ophthalmol Clin* 2009; **49**(2): 53–59.
15 Coffee RE, Jain A, McCannel TA. Ultra wide-field imaging of choroidal metastasis secondary to primary breast cancer. *Semin Ophthalmol* 2009; **24**(1): 34–36.
16 Shah SP, Jain A, Tsui I, McCannel TA. Optos Optomap Panoramic 200MA imaging of a serous choroidal detachment responsive to furosemide. *Semin Ophthalmol* 2009; **24**(1): 40–42.
17 Cheng SC, Yap MK, Goldschmidt E, Swann PG, Ng LH, Lam CS. Use of the Optomap with lid retraction and its sensitivity and specificity. *Clin Exp Optom* 2008; **91**(4): 373–378.
18 Kirkpatrick JN, Manivannan A, Gupta AK, Hipwell J, Forrester JV, Sharp PF. Fundus imaging in patients with cataract: role for a variable wavelength scanning laser ophthalmoscope. *Br J Ophthalmol* 1995; **79**(10): 892–899.
19 Neubauer AS, Yu A, Haritoglou C, Ulbig MW. Peripheral retinal changes in acute retinal necrosis imaged by ultra widefield scanning laser ophthalmoscopy. *Acta Ophthalmol Scand* 2005; **83**(6): 758–760.
20 Neubauer AS, Kernt M, Haritoglou C, Priglinger SG, Kampik A, Ulbig MW. Nonmydriatic screening for diabetic retinopathy by ultra-widefield scanning laser ophthalmoscopy (Optomap). *Graefes Arch Clin Exp Ophthalmol* 2008; **246**(2): 229–235.
21 Chou B. Limitations of the Panoramic 200 Optomap. *Optom Vis Sci* 2003; **80**(10): 671–672.
22 Jones WL. Limitations of the Panoramic 200 Optomap. *Optom Vis Sci* 2004; **81**(3): 165–166.

Supplementary Information accompanies the paper on Eye website (http://www.nature.com/eye)